Nanotechnology

PAPER

An effective and simple oxygen nanosensor made from MPA-capped water soluble CdTe nanocrystals

To cite this article: Pick Chung Lau *et al* 2013 *Nanotechnology* **24** 015501

View the article online for updates and enhancements.

Related content

- Thermally robust and blinking suppressed core/graded-shell CdSe/CdSe1-xSx/CdS ‘giant’ multishell semiconductor nanocrystals
  Pick Chung Lau, Zhaozhao Zhu, Robert A Norwood et al.
- The influence of capping thioalkyl acid on the growth and photoluminescence efficiency ofCdTe and CdSe quantum dots
  Fadi Aldeek, Lavinia Balan, Jacques Lambert et al.
- Highly efficient near-infrared light-emitting diodes by using type-II CdTe/CdSe core/shell quantum dots as a phosphor
  Huaibin Shen, Ying Zheng, Hongzhe Wang et al.

Recent citations

- Host–guest luminescent materials based on highly emissive species loaded into versatile sol–gel hosts
  Kassio P. S. Zanoni *et al*
- Reversed oxygen sensing using colloidal quantum wells towards highly emissive photoresponsive varnishes
  Monica Lorenzon *et al*
- Oxygen Sensitivity of Atomically Passivated CdS Nanocrystal Films
  Lorenzo Maserati *et al*

IOP | ebooks™

Bringing you innovative digital publishing with leading voices to create your essential collection of books in STEM research.

Start exploring the collection - download the first chapter of every title for free.

This content was downloaded from IP address 128.196.206.45 on 08/04/2019 at 22:49

IOP PUBLISHING NANOTECHNOLOGY

Nanotechnology **24** (2013) 015501 (8pp) doi:10.1088/0957-4484/24/1/015501

An effective and simple oxygen nanosensor made from MPA-capped water soluble CdTe nanocrystals

Pick Chung Lau, Robert A Norwood, Masud Mansuripur and Nasser Peyghambarian

College of Optical Sciences, The University of Arizona, Tucson, AZ 85721, USA

E-mail: pclau@email.arizona.edu, rnorwood@optics.arizona.edu, masud@optics.arizona.edu and nnp@u.arizona.edu

Received 23 August 2012, in final form 23 October 2012
Published 5 December 2012
Online at stacks.iop.org/Nano/24/015501

Abstract

CdTe semiconductor nanocrystals (NCs) with 3-mercaptopropionic acid as the ligand exhibit a reversible response towards inter-switching oxygen and argon environments. The photoluminescence response is investigated at multiple oxygen concentrations, NC coverage and excitation intensities, in which all conditions exhibit full recovery upon exposure to flowing argon. The CdTe NC's large surface-to-volume ratio results in high sensitivity towards oxygen molecules with significant photoluminescence quenching at a concentration of 40 ppm. This suggests a novel approach to the creation of simple, inexpensive and ultrasensitive oxygen nanosensors.

(Some figures may appear in colour only in the online journal)

1. Introduction

One of the very appealing and unique properties of semiconductor nanocrystals (NCs) is their size dependent electronic structure. With typical dimensions of 1–10 nm, these nanocrystals bridge the gap between molecules and bulk crystals. As the size of the particle increases, the separation of the energy levels decreases. Due to the exquisite nature of these nanomaterials, much effort has been devoted to understanding the spectral diffusion, blinking and photobleaching behavior of NCs under various conditions (temperature, ambience, type of NC, etc) [1, 2, 7, 10].

However, research on making NCs respond reversibly to environmental changes remains incomplete. Previously, Amjad *et al* [4] demonstrated that CdSe nanocrystals are capable of responding to specific environments in a reversible and rapid fashion, but the photoluminescence (PL) of CdSe NCs was not found to be reversible once the NCs were exposed to alternating oxygen and argon environments. This limits the applicability of CdSe NCs serving as oxygen nanosensors. Due to the fact that the oxygen sensor is a common and important piece of probing equipment in the biological, aerospace, chemical and environmental fields [15–18], the ability to make oxygen nanosensors using NCs is a desirable goal that could serve as a platform to bring sensing towards the next level in terms of size, simplicity and ultra-high oxygen sensitivity.

Here, we report on the PL properties of water soluble CdTe NCs with 3-mercaptopropionic acid as the ligand, showing that these NCs are capable of responding reversibly to an inter-switching of the oxygen and argon environments over multiple hours of photoexcitation. These NCs quench upon exposure to oxygen, but when the system is purged with argon their PL revives to the original intensity. Due to the fact that these colloidal NCs have a large surface-to-volume ratio, they are extremely sensitive to oxygen molecules in their environment. As reported in our findings, CdTe NCs quench significantly even at an O_2 concentration of 40 ppm. This behavior has the side benefit of providing simple, inexpensive, and ultrasensitive oxygen nanosensors.

2. Procedure

2.1. Chemicals

The chemicals used were cadmium nitrate tetrahydrate, purum >99.0% (Sigma Aldrich, 20911), tellurium pow-

© 2013 IOP Publishing Ltd Printed in the UK & the USA

der, 200 mesh, 99.8% (Sigma Aldrich, 266418), 3-mercaptopropionic acid (MPA) >99% (Sigma Aldrich, M580-1), sodium borohydride, powder >98% (Sigma Aldrich 452882), N^1-(3-trimethoxysilylpropyl)diethylenetriamine (DETAS)—technical grade (Sigma Aldrich, 413348), hydrogen peroxide, 50 wt% (Sigma Aldrich, 516813), and sulfuric acid, 99.999% (Sigma Aldrich, 339741).

2.2. Synthesis of NaHTe precursor solution

The following procedure was used to synthesize NaHTe precursor solution. 50.8 mg of tellurium powder was added to a 100 ml three-neck flask followed by 37.8 mg of sodium borohydride. The flask was then purged with argon gas for at least 5 min. Subsequently, 10 ml of argon saturated distilled (DI) water was injected into the flask via a 15 ml syringe. The three-neck flask was then immersed in an 80 °C water bath for at least 30 min.

2.3. Synthesis of CdTe + MPA NCs

The method was based on the procedure developed by Zou Lei *et al* [6, 8, 9]. In short, 40 ml of argon saturated DI water was inserted into a 100 ml three-neck flask. It was followed by insertion of 0.2 mmol of Cd^{2+} precursor solution (previously prepared by dissolving cadmium nitrate tetrahydrate in DI water). 0.34 mmol of 3-mercaptopropionic acid was then added into the solution. Subsequently, the pH was adjusted to 11.9 by drop-wise addition of NaOH. Under stirring, 0.02 mmol of freshly prepared NaHTe was swiftly injected into the solution. The temperature was then gradually increased using an oil bath to 100 °C. NCs were grown for 25 min. At this point, a total of 0.4 mmol of MPA was added gradually within a period of 5 min. CdTe + MPA q-dots were then grown for another 45 min before samples were taken. The resulting q-dots had their peak photoluminescence at 615 nm.

2.4. Preparation of CdTe + MPA NC thin film samples

VWR VistaVision cover slips (0.16–0.19 mm thickness) were used as the glass substrate to attach the NCs. These cover slips were first piranha etched (1:3 by volume hydrogen peroxide to sulfuric acid) for 30 min. The cover slips were then immersed in 2% 3-aminopropyltriethoxysilane (APTES) solution in ethanol for 1 h at 70 °C. A very dilute NC solution (dilution factor of 1.2×10^4 with reference to an optical density of 0.4 at 473 nm) was later spin coated onto the cover slip. The cover slips were subsequently washed with flowing DI water to remove any excess NCs that were weakly attached through ionic interactions. The remaining NCs that were attached to the APTES via zwitter-ionic bonds were dried on a 50 °C hot plate. The samples were then dried at room temperature for another 24 h.

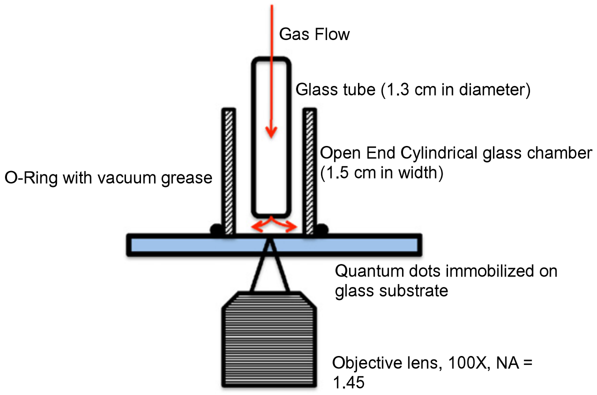

Figure 1. The system setup for measuring the CdTe NC PL with gas flow. The PL of the NCs was collected from the same reflected path towards the EMCCD.

2.5. Fluorescence microscope

All photoluminescence measurements were carried out under a wide field fluorescence microscope (Zeiss Axio Imager Z2). The NC sample was mounted such that the gas line was placed within 1 mm above the surface with a fixed flow rate of 5 lpm (figure 1). The gas line was premixed with the proportion of interest using a digital mass flow controller (Sierra Instruments C101-DD-2, range 0.2–10 sccm) for the oxygen source and a flow meter (Matheson, range 0.5–25 lpm) for the argon source. The photoluminescence of the NCs was collected by an oil immersion 100× objective lens (NA = 1.45) and detected by an air-cooled EMCCD camera (Photonmax 512B) after passing an emission bandpass filter at 605 ± 15 nm. The exposure time was fixed at 2 s. The camera background values were measured and accounted for in all PL measurements. A mercury arc lamp (HBO 100) was used as the source, and the excitation wavelength was fixed at 405 nm. The maximum irradiance was measured at around 12 W cm^{-2}.

2.6. AFM measurement

AFM (Agilent 5500) measurements were conducted on the NC immobilized cover slip over a 5×5 μm^2 area or a 10×10 μm^2 area; the tapping mode was used.

2.7. TEM measurement

All NCs were measured using a Hitachi-8100 TEM. The samples were placed on an ultrathin carbon film on a 400 mesh copper grid (Ted Pella-01822).

3. Results and discussion

Over the past few years, various NC systems have been shown to exhibit excellent photostability under inert environmental conditions [2, 5]. However, there has generally been little study of whether the changes in the photoexcitation properties induced by the environment are reversible. Here we report

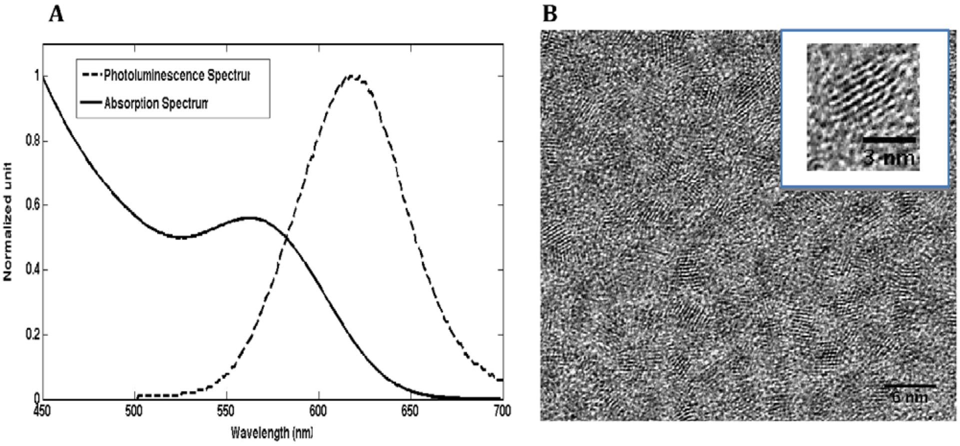

Figure 2. (A) Absorption and emission spectra of the CdTe NCs. These specific water soluble NCs have peak emission at 615 nm and peak absorption at 565 nm. The emission spectrum has an FWHM of 70 nm, consistent with the value found by Zou Lei *et al* [6]. The broader emission FWHM is due to the ultrafast fabrication method. The quantum yield was measured to be 56% in comparison to the standard organic dye molecule Rhodamine 6G. (B) HRTEM measurements were conducted on the water soluble NCs. The sample had an average size of 3.45 nm in diameter, similar to that predicted by Yu *et al* [19] to within 10% error. The %RMS in diameter was estimated to be around 15%. The inset shows a zoomed-in view of one of the particles. The shape of the particle is slightly prolate with an aspect ratio of 1.1.

that CdTe NCs with MPA as ligands have a reversible PL response as alternation occurs between oxygen and argon environments. We also investigated the kinetics of NCs at multiple oxygen concentrations and excitation intensities.

First of all, photoluminescence spectrum, absorption spectrum and HRTEM measurements were performed to understand the general characteristics of water soluble CdTe NCs. The summarized results are shown in figure 2.

In addition, CdTe + MPA NCs are extremely stable under an inert environment. Figure 3 shows the time dependent photoluminescence results for CdTe NCs under multiple excitation irradiances (0.6–12 W cm^{-2}). Consistent with the observations made by Amjad *et al* [4], we found the aqueous-based CdTe NCs to show no signs of decay under an inert environment. We note that water-based CdTe+MPA NCs provide us with a cost effective and biologically compatible route to ultrastable nanostructures, in contrast to standard organic solvent-based techniques.

We then exposed the CdTe NCs alternately to argon and oxygen gases. In contrast to the conventional method of mounting the sample in a sealed flow chamber, our CdTe NCs were directly purged with the flowing gas of interest at a flow rate of 5 lpm at a temperature of 25 °C. As shown in figure 4, the CdTe NCs, upon bleaching with 160 ppm oxygen in argon mixture at a flow rate of 5 lpm, can be revived multiple times by purging with 100% argon. The NCs have large transition dipole moments and they transfer their absorbed photo-induced energy to any neighboring oxygen molecules to form singlet oxygen species. These highly reactive molecules can then adsorb to NC surfaces and therefore create trap sites that would inhibit radiative recombination [3, 13]. The fact that the CdTe NCs fully recover after being bleached in oxygen is a strong indication that the oxygen bonding to the surface is reversible.

An interesting finding is that NCs undergoing successive attempts at recovery exhibit steadily brighter PL and eventually approach 100% recovery. It was believed at first that the higher PL counts were caused by elevated background values due to continuous camera exposure that created undesirable charging. However, the measured background value increased by less than 1% after 5 h of exposure at 2 W cm^{-2} of irradiance. This implies that the enhanced PL recovery must have come from the photoexcited nanocrystals themselves. After each recovery cycle, the oxygen affinity towards the NCs reduces. We believe that the residual water molecules surrounding the ligands have been evaporated by convection of the argon flow, thus reducing the possibility of any oxidation induced by water molecules [12, 14]. The argon gas tank used was of industrial grade, where the moisture content was less than 5 ppm [20, 21]. Therefore, one would expect the moisture content within the gas flow chamber to be gradually conforming under convection to within the same order of magnitude of 5 ppm from an average

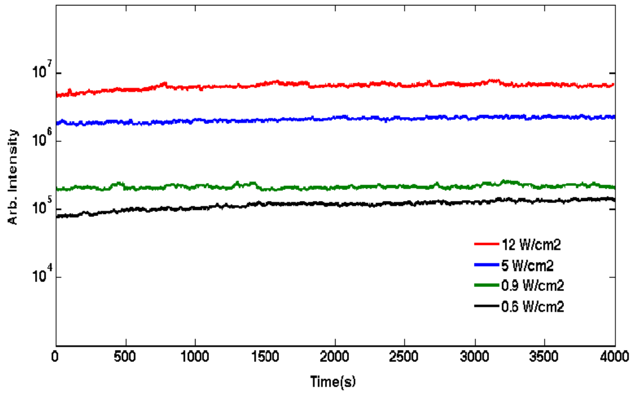

Figure 3. The CdTe nanocrystals were exposed to multiple fluences from 0.6 to 12 W cm^{-2} under argon flow, yet there was no sign of decay over a period of 1 h. The slight increase in some of the trajectories could be caused by thermal or source irradiance fluctuations.

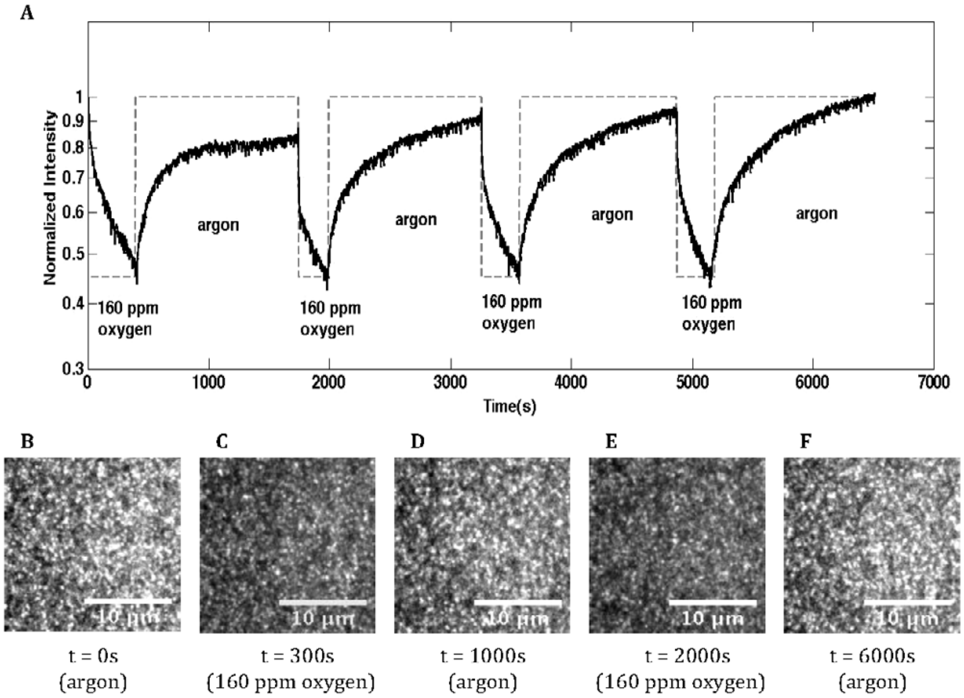

t = 0s (argon)

t = 300s (160 ppm oxygen)

t = 1000s (argon)

t = 2000s (160 ppm oxygen)

t = 6000s (argon)

Figure 4. (A) The PL trajectory of CdTe NCs immobilized on a glass substrate that were alternately exposed to 160 ppm oxygen and 100% argon at a constant flow rate of 5 lpm. The irradiance was fixed at 2 W cm^{-2} at 405 nm and the NC coverage was about 15 NCs μm^{-2}. (B)–(F) Pictures of photoexcited CdTe NCs under different conditions as observed by the EMCCD camera with an emission filter of 605 nm ± 15 nm.

relative humidity of 40%. It would be desirable to be able to directly measure the relative humidity within the chamber but, due to limitations in the equipment, the moisture content profile is currently not available. Therefore, more research is needed to better understand the causes of the increased photoluminescence.

We investigated the photobleaching behavior of the CdTe NCs at various oxygen concentrations along with their recovery behavior. The NCs were initially photobleached at various oxygen concentrations for 10 min, as shown in figure 5. Once the atmosphere was switched back to argon, the sample's PL recovered rapidly and came to within 98% of the original PL at the end of the hour.

The decay curve can be best fitted by a double exponential (figure 6), which is consistent with the findings of other research groups [11, 12]. Initially, the strong-exponential decay (α parameter) takes precedence over the weaker decay rate (β parameter). This happens because there is a large surface availability for interactions between NCs and oxygen molecules. Due to the fact that there is no mediating material between the atmosphere and the NCs, oxidation is almost instantaneous. The α value shows no significant change across the investigated oxygen concentrations (40–2000 ppm), with an average value of approximately 0.026 ± 0.003 s^{-1}.

The weaker decay parameter (β) can be explained by oxygen diffusion into the inner cluster of the NCs. Although the functionalized glass substrate was intended to create a homogeneous distribution of individual NCs, a large fraction of these nano-particles formed small clusters because of charge-to-charge aggregation during deposition, as evidenced from the AFM measurements shown in figure 7. As a result, interactions between oxygen molecules and NCs were hampered by the presence of intermediate nanomaterials. An empirical expression relating the β parameter to the O$_2$ concentration, $[C]$, in ppm is given by

$$\beta = 4.16 \times 10^{-5}[C]^{0.4458}.$$

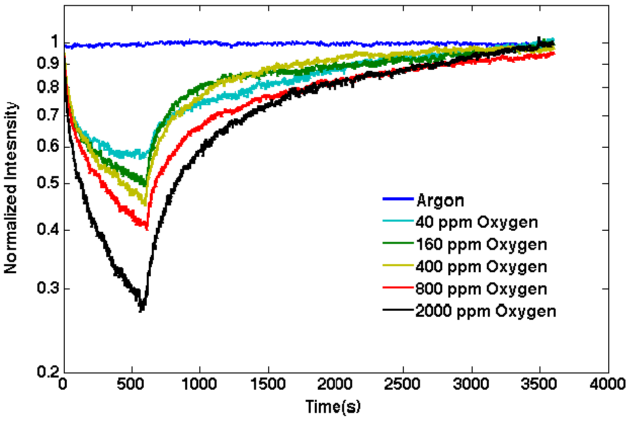

Figure 5. PL decay and recovery of CdTe NCs for various oxygen concentration at 5 lpm flow rate. The excitation intensity was fixed at 2 W cm^{-2} at 405 nm.

The PL recovery rates have a more complex behavior. As shown in figure 5, at $t = 600$ s, the NCs were immediately purged with 100% argon. All recovery curves exhibited the

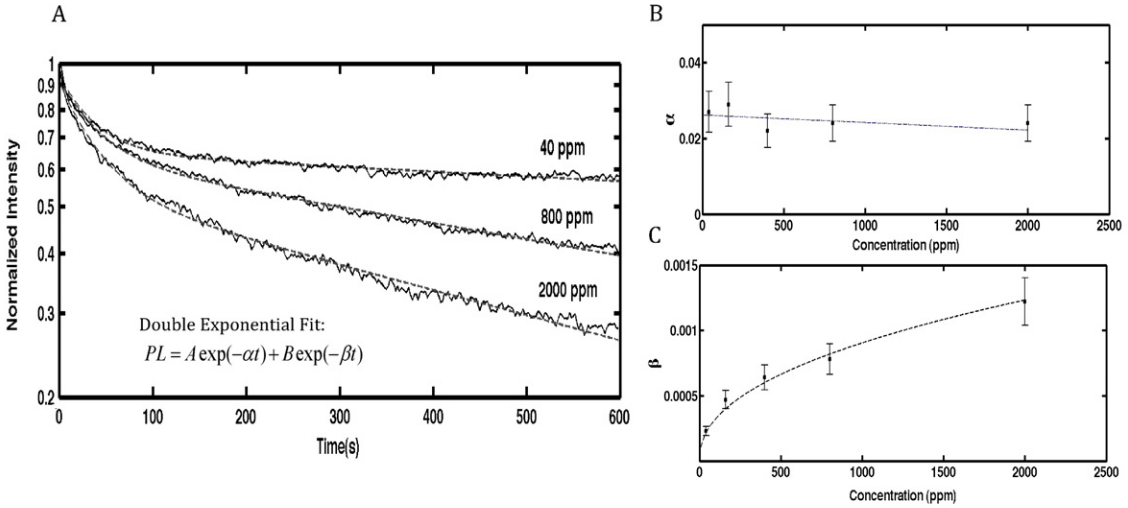

Figure 6. (A) A close-up view of the PL decay curves at multiple oxygen concentrations, superimposed on double-exponential fitting curves. The *R*-squared value for each fit is greater than 0.95. (B)–(C) The fitting parameters of the first and second exponentials (α and β) as functions of the oxygen concentration.

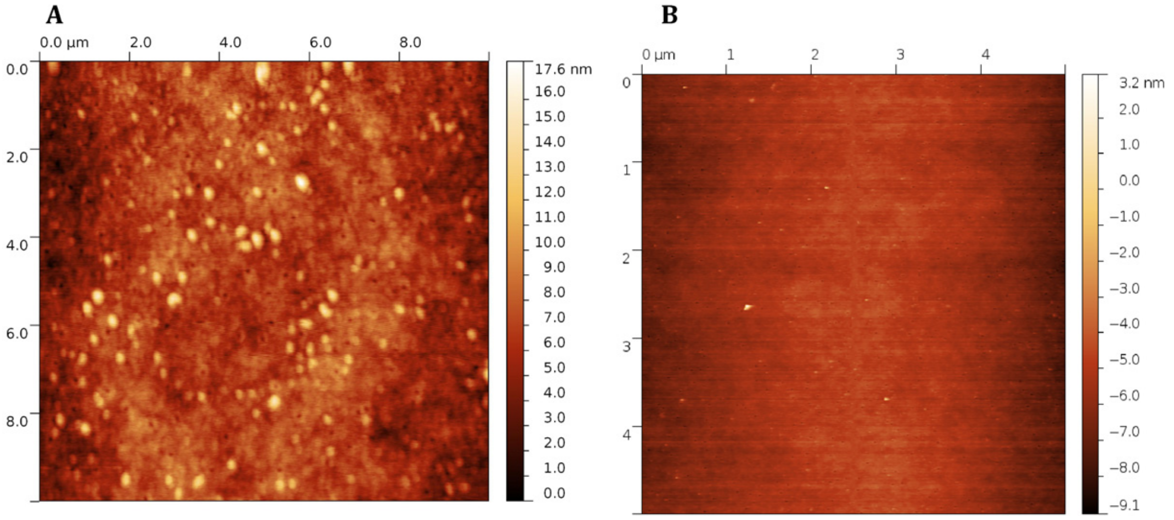

Figure 7. (A) AFM measurement on a borosilicate cover glass with an NC coverage of approximately 15 NCs $\mu\mathrm{m}^{-2}$. NC clustering is evident from the height profile. The clusters have a height of about 17 nm, which is 5 times the height of a single NC. In contrast, the AFM image in (B) shows a separate substrate that was prepared with a coverage of less than 0.1 NC $\mu\mathrm{m}^{-2}$, and the height of each nano-particle is about 3.5 nm, consistent with the size obtained from TEM images. It is evident, therefore, that the NCs in (A) have formed small clusters that could account for the weaker decay parameter (β) of the double-exponential fit.

following saturation pattern with an $R^2 > 0.95$:

$$\mathrm{PL} = \frac{at}{b+t} + ct + d.$$

The PL in general has a rapid initial rise followed by an increase at a much slower rate. This is expected because the outermost NCs in a cluster are the first to be purged with argon; they thus exhibit the quickest recovery. As argon diffuses into the inner clusters, more oxygen molecules are eliminated but at a much lower rate. The initial recovery is largely exemplified by the b parameter. Similarly to the α value in the PL decay kinetics, the b parameter is not strongly dependent on the oxygen concentration; it changes by at most about 20% across a 50-fold increase of oxygen concentration (table 1).

The c parameter, which describes the slow recovery rate, has a change of close to an order of magnitude over the full range of oxygen concentrations under study. The c parameter is small at low oxygen levels and increases upon passing the 400 ppm mark. The reason for this behavior is still unknown; more studies are needed to clarify the intrinsic kinetics of NCs in the presence of oxygen molecules. In addition, the fact that the c parameter does not converge to zero is perhaps an indication of the incompleteness of the model. More work is needed to understand the PL recovery over extended periods of time.

A separate experiment (figure 8) was conducted where an ensemble of NCs was photobleached over 30 min, which is 3 times longer than the decay time of our previous investigation

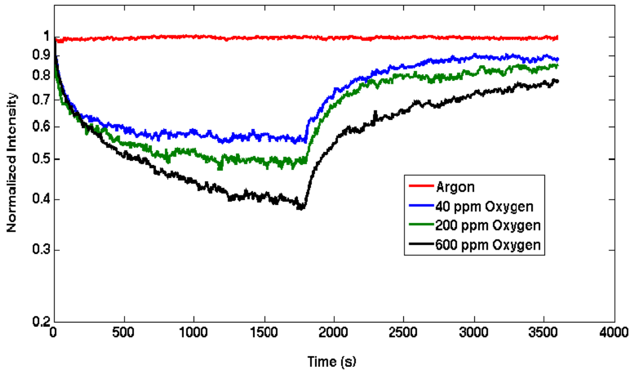

Figure 8. PL decay and recovery of CdTe NCs with an average coverage of 15 NCs μm^{-2}. The CdTe NCs were photobleached at various oxygen concentrations for 30 min before switching over to argon. All gas flow was maintained at 5 lpm.

Table 1. Fitting parameters for PL under recovery at various oxygen concentrations.

O_2 concentration (ppm)	a	b (s)	c (s^{-1})	d
40	0.22	319.8	7.19×10^{-5}	0.59
160	0.36	320.5	2.49×10^{-5}	0.57
400	0.53	345.6	5.00×10^{-6}	0.49
800	0.42	349.7	5.07×10^{-5}	0.42
2000	0.55	393.8	7.30×10^{-5}	0.29

Table 2. Double-exponential fitting parameters at increasing oxygen concentration.

O_2 concentration (ppm)	A	α (s^{-1})	B	β (s^{-1})	A/B
40	0.29	0.027	0.65	0.000 23	0.45
160	0.28	0.029	0.66	0.000 47	0.42
400	0.29	0.022	0.66	0.000 64	0.43
800	0.30	0.024	0.63	0.000 78	0.47
2000	0.37	0.024	0.55	0.001 22	0.68

shown in figure 5. Observations were conducted under various oxygen concentrations and these NCs were subsequently recovered under argon flow for 30 min.

For longer photobleaching durations, the PL decay patterns are very similar to our previous attempts to within 5–10% relative error in the first 10 min. This indicates good repeatability for our NC sensing system. The 40 ppm oxygen decay curve reaches a steady state of 60% normalized intensity, which is similar to the 10 min decay curve that also converges at about 60%, as shown in figure 5. However, as we approach higher oxygen concentration, the final decay point becomes much lower due to the stronger β parameter in the double-exponential fit mentioned in table 2. However, we observed that as the photobleaching duration becomes longer, the NC recovery rate reduces. With a 30 min recovery time frame, our previous experiment (with 10 min photobleaching) yields an 86%–93% recovery across a varying oxygen concentration range from 40 to 2000 ppm (figure 5). However, for the case of longer photobleaching times (figure 8), the NCs only recover to within 75%–84%. It is possible that we could understand the photooxidation as a process of oxygen adsorption into the inner structure of the NCs. As the decay duration becomes longer, oxygen molecules get trapped within the NCs inner core. Therefore, it is harder for the argon to remove any residual oxygen present within the NCs. Hence, we observed a lower recovery rate. Furthermore, we found that the recovery of all three oxygen concentration plateaus was in the region of 90%. The fact that we are 10% short of full recovery indicates that there is some permanent photobleaching that it is impossible for the use of argon flow to recover because of the penetration depth of the oxygen molecule that prevents the argon from removing it. More research is needed to find the exact mechanism of photobleaching and recovery.

The NCs' PL response at low coverage (~0.1 NC μm^{-2}) was also investigated (figure 9). Due to the fact that colloidal NCs blink, measurement of the PL decay at ultralow oxygen concentrations becomes very difficult. As a result, meaningful data can only be collected when the NCs are inter-switched between argon and air. As expected, the PL decay and recovery become almost a binary response, as evidenced in the PL trajectory depicted in figure 9. The excitation irradiance was fixed at 0.6 W cm^{-2}. This confirms the fact that CdTe + MPA NCs at a single particle level can fully recover multiple times with no signs of photobleaching over a period of 2 h. In contrast to high NC coverage, the recovery for low NC coverage was almost instantaneous because of the absence of clusters discussed in conjunction with figure 7(B).

We also investigated the PL decay of CdTe NCs at varying levels of the incident radiation. As can be seen in figure 10, the power was increased from 0.6 to 12 W cm^{-2}, with the excitation wavelength fixed at 405 nm and the oxygen concentration kept at 160 ppm. As expected, photo-induced oxidation occurs more rapidly at higher UV light fluence due to the increasing probability of interaction between the NCs and singlet oxygen. Under all circumstances, we found the PL decay to be reversible. Upon switching to an argon gas flow, the recovery was rapid and reached a plateau at the end of the hour. The slight overshoot in the case of 12 W cm^{-2} could be due to a slight increase of irradiance during operation at this maximal power level.

4. Conclusion

In summary, we have demonstrated that CdTe semiconductor nanocrystals with MPA ligands exhibit reversible PL behavior upon switching between oxygen and argon gas over multiple hours of continuous excitation. Significant PL decay was observed at ultralow oxygen concentrations (40 ppm), and the decay kinetics was experimentally determined at multiple oxygen concentrations and excitation intensities. However, more research is needed on the spectral evolution of NCs on film during inter-switching between argon and oxygen environments. Wilfried *et al* [2] have attempted this experiment and upon photooxidation the PL spectrum of organic solvent-based CdSe NCs was blue shifted. It would be very interesting if the spectral properties of water soluble

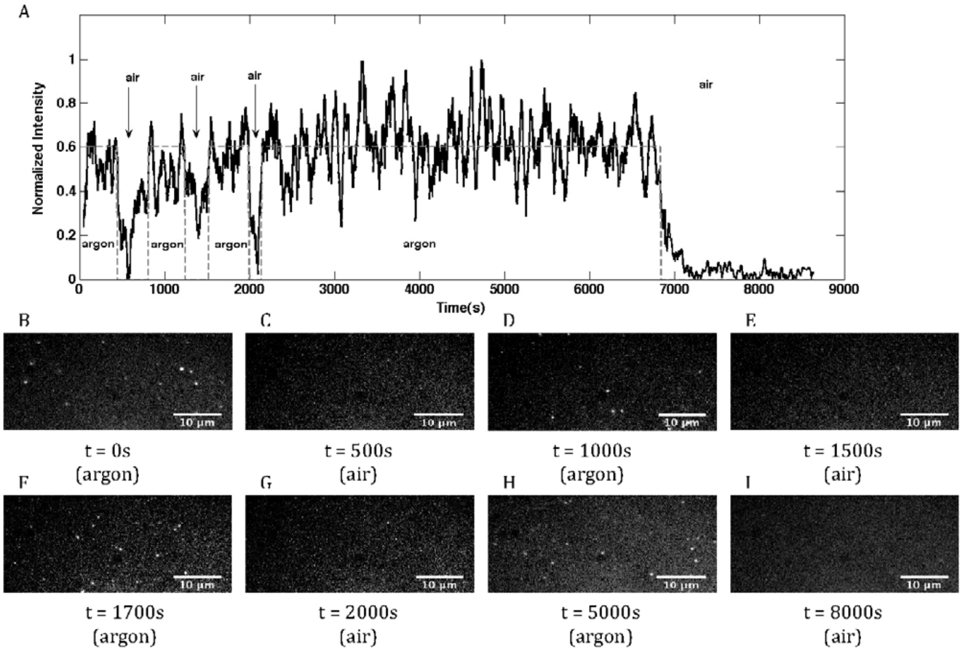

t = 0s (argon)

t = 500s (air)

t = 1000s (argon)

t = 1500s (air)

t = 1700s (argon)

t = 2000s (air)

t = 5000s (argon)

t = 8000s (air)

Figure 9. (A) The photoluminescence trajectory of CdTe NCs at approximately 0.1 NC μm^{-2} excited at 405 nm with a UV irradiation fluence of 0.7 W cm^{-2}. At low NC coverage, these nano-particles exhibit an almost binary PL response towards alternation between argon gas and air. (B)–(I) Pictures of photoexcited CdTe NCs under different conditions as observed by the EMCCD camera with an emission filter of 605 nm ± 15 nm.

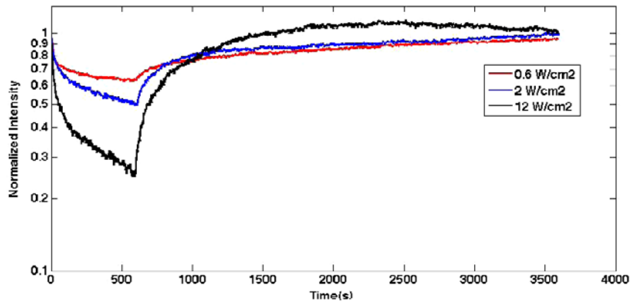

Figure 10. Photoluminescence trajectories of CdTe NCs at an areal coverage of 15 NCs μm^{-2} at various UV illumination intensities. The NCs were initially exposed to 160 ppm oxygen at 5 lpm and subsequently recovered under argon gas flow.

NCs were to exhibit reversible spectral shifting under argon and oxygen environments. In addition, to better understand the photostability of water soluble CdTe NCs, a time correlated photon counting method can be applied to measure the fluorescence lifetime changes of NCs exposed under argon and oxygen environments. Furthermore, it remains uncertain whether water soluble NCs photobleach only in the presence of oxygen. It is demonstrated that oxygen is a necessary factor of photobleaching, but it may not be a sufficient cause. It is not doubted that water molecules do affect the photoluminescence [12, 14], and therefore a more complete study is needed to relate the moisture content with the PL trajectories. Moreover, based on previous studies by Amjad *et al* [4], organic solvent CdSe NCs respond reversibly towards the presence of triethylamine and benzylamine; as a result, an understanding of the responses of water soluble CdTe NCs towards these gases could help us to better understand the potential of water soluble CdTe NCs serving as nanosensors.

Acknowledgment

This work was supported in part by the DARPA ZOE program (Grant no. W31P4Q-09-1-0012).

References

[1] Lee S F and Osborne M A 2009 Brightening, blinking, bluing and bleaching in the life of a quantum dot: friend or foe? *Chem. Phys. Chem.* **10** 2174–91

[2] van Sark W G J H M *et al* 2001 Photooxidation and photobleaching of single CdSe/ZnS quantum dots probed by room-temperature time-resolved spectroscopy *J. Phys. Chem.* B **105** 8281–4

[3] Ma J *et al* 2006 Photostability of thiol-capped CdTe quantum dots in living cells: the effect of photo-oxidation *Nanotechnology* **17** 2083–9

[4] Amjad *et al* 2003 Photoactivated CdSe nanocrystals as nanosensors for gases *Nano Lett.* **3** 819–22

[5] Felix K, Alf M and Thomas B 2001 Oxygen-induced blinking of single CdSe nanocrystals *Adv. Mater.* **13** 672–6

[6] Zou L *et al* 2008 Ultrafast synthesis of highly luminescent green- to near infrared-emitting CdTe nanocrystals in aqueous phase *J. Mater. Chem.* **18** 2807–15

[7] Chen H P, Gai H and Yeung E S 2009 Inhibition of photobleaching and blue shift in quantum dots *Chem. Commun.* 1676–8

[8] He H *et al* 2006 Single nonblinking CdTe quantum dots synthesized in aqueous thiopropionic acid *Angew. Chem.* **118** 7750–3

[9] Liu Y F 2009 Selective synthesis of CdTe and high luminescence CdTe/CdS quantum dots: the effect of ligands *J. Colloid Interface Sci.* **333** 690–8

[10] Larson D R 2003 Water-soluble quantum dots for multiphoton fluorescence imaging *in vivo Science* **300** 1434–6

[11] Shu G W *et al* 2005 Photoluminescence of colloidal CdSe/ZnS quantum dots under oxygen atmosphere *IEEE Trans. Nanotech.* **4** 632–6

[12] Cordero S R *et al* 2000 Photo-activated luminescence of CdSe quantum dot monolayers *J. Phys. Chem.* B **104** 12137–42

[13] Charon G *et al* 2012 Insights into the mechanism of quantum dot-sensitized singlet oxygen production for photodynamic therapy *J. Phys. Chem.* C **116** 9334–42

[14] Zhang Y *et al* 2006 Time-dependent photoluminescence blue shift of the quantum dots in living cells: effect of oxidation by singlet oxygen *J. Am. Chem. Soc.* **128** 13396–401

[15] Ramamoorthy R, Dutta P K and Akbar S A 2003 Oxygen sensors: materials, methods, designs and applications *J. Mater. Sci.* **38** 4271–82

[16] Lessner F H, Jennings M E, Hirata A, Duin E C and Lessner D J 2012 Subunit D of RNA polymerase from methanosarcina acetivorans contains two oxygen-labile (4Fe–4S) clusters: implications for oxidant-dependent regulation of transcription *J. Biol. Chem.* **287** 18510

[17] Kortzinger A and Schimanski J 2005 High quality oxygen measurements from profiling floats: a promising new technique *J. Atmos. Ocean. Technol.* **22** 302–8

[18] Lin H W *et al* 2012 Novel oxygen sensor based on terfluorene thin-film and its enhanced sensitivity by stimulated emission *J. Mater. Chem.* **22** 13446–50

[19] Yu *et al* 2003 Experimental determination of the extinction coefficient of CdTe, CdSe, and CdS nanocrystals *Chem. Mater.* **15** 2854–60

[20] Matheson, Argon www.mathesongas.com/pdfs/products/Argon-Pure-Gas.pdf

[21] Matheson, Oxygen www.mathesongas.com/pdfs/products/Oxygen-Pure-Gas.pdf